Progress In Electromagnetics Research B, Vol. 24, 63–78, 2010

IMPACT OF DIMENSIONAL PARAMETERS ON MUTUAL INDUCTANCE OF INDIVIDUAL TOROIDAL COILS USING ANALYTICAL AND FINITE ELEMENT METHODS APPLICABLE TO TOKAMAK REACTORS

M. R. Alizadeh Pahlavani and A. Shiri

Department of Electrical Engineering
Iran University of Science and Technology (IUST)
Tehran, Iran

Abstract—A toroidal field coil (TFC) is composed of several individual toroidal coils (ITCs), which are connected in a series and distributed in a toroidal and symmetrical form. Cross section of ITCs is rectangular or negligible. This paper presents analytical equations for mutual inductance of two ITCs applicable to Tokamak reactors using the filament method. These equations are based on those formulated by Neumann. The numerical analysis of the integrations resulting from these equations is solved using the extended three-point Gaussian algorithm. The finite element method (FEM) is employed to verify the mutual inductance equations of ITCs. The results obtained using the FEM, when dimensional parameters of ITCs are changed, confirm the analytical and empirical results showing an error of less than 0.2043% in the worst case. This indicates the reliability of the presented equations.

1. INTRODUCTION

Different coils in the area of superconductor magnetic energy storage (SMES), nuclear fusion reactors, and Tokamak reactors have been studied [1]. As an example, all Tokamak reactors have an array of TFC, poloidal field coil (PFC), and central solenoid coil (CSC). The TFC is composed of several ITCs connected in a series and distributed in a toroidal and symmetrical form. The magnetic field line is created by a combination of TFC, PFC and a toroidal plasma current. Note that a helical toroidal coil (HTC) can create the magnetic field line, as

Received 12 June 2010, Accepted 26 July 2010, Scheduled 4 August 2010
Corresponding author: M. R. Alizadeh Pahlavani (Mr_Alizadehp@iust.ac.ir).

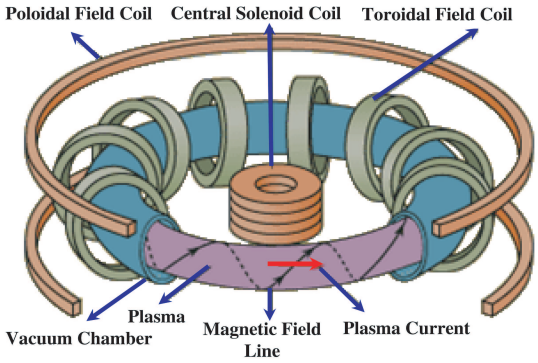

Figure 1. The magnetic part of a Tokamak reactor.

well [2–7]. The CSC is used to drive the toroidal plasma current in a Tokamak reactor. The magnetic part of a Tokamak reactor is shown in Fig. 1. As seen in this figure, each of TFC, PFC, and CSC is composed of several ITCs which are distributed in different forms. The capability of modular implementation of the TFC is one of its main advantages over the HTC [8].

An inductive link consists of two ITCs, forming a loosely coupled transformer. An ITC consists of several coaxial circular rings. Each ring of an ITC has an inductive link with a ring of another ITC, and there is a mutual inductance between them. In this paper, all of the rings belong to the first and the second ITCs are called primary and secondary rings, respectively. Each primary ring (in the first ITC) generates a magnetic field that is partly picked up by the secondary ring (in the second ITC). In this way, the power can be transferred wirelessly. The decrease in power transfer efficiency of the inductive power system is caused by lower mutual inductance due to misalignment of the rings. Therefore, in the equations of the mutual inductance between two rings, misalignments have to be taken into consideration. Many investigations have been done in the literature to the problem of mutual inductance calculation for coaxial circular coils [9–15]. These contributions have been based on the application of Maxwell's formula, Neumann's formula, and the Biot-Savart law. The mutual inductance of coaxial circular rings can be obtained in analytical or semi-analytical forms expressed by elliptical integrals of the first, second, and third kind, Heuman's Lambda function, Bessel functions, and Legendre functions [16–18]. However, the calculation of the mutual inductance of non-coaxial circular rings is of fundamental practical interest to electrical engineers and physicists. In this paper,

we will present the mutual inductance between two inclined ITCs when either their axes intersect at the center of one of the ITCs or their axes intersect but not at the center of one of them. This is accomplished using complete elliptic integrals of the first and the second kind. Also, we will use the filament method [19–28] to calculate the mutual inductance between two ITCs. These ITCs may have any cross-section. Note that the analytical equations are purely 3-D because ITCs' axes may be coaxial or non-coaxial. In this paper, we use extended three-point Gaussian numerical integration to solve the presented equations. They are validated using the FEM.

This paper is organized as follows: In Section 2, analytical equations are presented to calculate the mutual inductance between two inclined rings when either their axes intersect at the center of one of the rings or their axes intersect but not at the center of one of them. In Section 3, analytical equations are presented to calculate the mutual inductance between two inclined ITCs when either their axes intersect at the center of one of the ITCs or their axes intersect but not at the center of one of them. In Section 4, the analytical results of Sections 2, and 3 are compared with the FEM results. Finally, in this section, magnetic flux density of two series ITCs is demonstrated.

2. ANALYTICAL EQUATION FOR MUTUAL INDUCTANCE BETWEEN TWO RINGS

In this section, the analytical equation for mutual inductance between two inclined circular rings is presented (see Fig. 2).

This equation is derived using Neumann's equation and is solved using complete elliptic integrals of the first and the second kind and the numerical integration method. The numerical integration method is based on the extended three point Gaussian algorithm [29]. The mutual inductance between two filamentary circular rings with inclined axes, one with radius R_{ph}, and another with radius R_{sl}, whose centers are not on the same axis, can be calculated as:

$$M = \frac{\mu_0}{\pi}\sqrt{R_{ph}R_{sl}} \cdot \int_0^{\pi} \left[\cos\theta - \frac{y_p}{R_{sl}}\cos\varphi\right] \Psi(k_r) V_r^{-1.5} d\varphi \tag{1}$$

where

$$V_r = \sqrt{1 - \cos^2\varphi \sin^2\theta - 2\frac{y_p}{R_{sl}}\cos\varphi\cos\theta + \left(\frac{y_p}{R_{sl}}\right)^2} \tag{2}$$

$$\alpha_r = \frac{R_{sl}}{R_{ph}}, \quad \beta_r = \frac{c_{gp}}{R_{ph}}, \quad k_r^2 = \frac{4\alpha_r V_r}{(1+\alpha_r V_r)^2 + \xi_r^2} \tag{3}$$

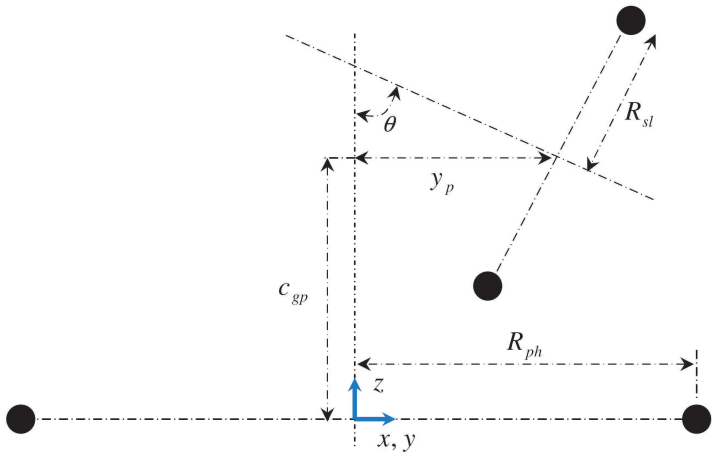

Figure 2. Two inclined filamentary circular rings (axes intersect but not at the center of either).

$$\xi_r = \beta_r - \alpha_r \cos\varphi \sin\theta \tag{4}$$

$$\Psi(k_r) = \left(\frac{2}{k_r} - k_r\right) K(k_r) - \frac{2}{k_r} E(k_r) = Q_{1/2}(x_r), \quad x_r = \frac{2 - k_r^2}{k_r^2} \tag{5}$$

R_{ph} the radius of the primary ring (larger ring);
R_{sl} the radius of the secondary ring (smaller ring);
c_{gp} the latitudinal distance between rings' centers;
y_p the longitudinal distance between rings' centers;
θ the angle between ring's axes;
$K(k_r)$ the complete elliptic integral of the first kind;
$E(k_r)$ the complete elliptic integral of the second kind;
$Q_{1/2}(x_r)$ Legendre function of the second kind and half-integral degree;
$\mu_0 = 4\pi \times 10^{-7}$ H/m the magnetic permeability of the vacuum.

3. ANALYTICAL EQUATION FOR MUTUAL INDUCTANCE BETWEEN TWO ITCS

For the calculation of the mutual inductance between all inclined circular rings of two inclined circular ITCs either with rectangular or negligible cross section, we use the well-known filament method and Equation (1). In the following calculations, we take into consideration

two ITCs when either their axes intersect at the center of one of the ITCs (Case I) or their axes intersect but not at the center of one of them (Case II). Note that Case II is a global state of Case I. Fig. 3 shows Case II where the secondary ITC is inclined. In this paper, the cross sections of the primary and the secondary ITCs are considered rectangular. The symbols in this figure are as follows:

R_p the average radius of the rings of the primary ITC (larger ITC);

R_s the average radius of the rings of the secondary ITC (smaller ITC);

W_p the width of the cross section of the primary ITC;

L_p the length of the cross section of the primary ITC;

W_s the width of the cross section of the secondary ITC;

L_s the length of the cross section of the secondary ITC;

c the latitudinal distance between ITCs' centers;

d the longitudinal distance between ITCs' centers;

θ the angle between ITCs' axes;

R_{pin} the inner radius of the primary ITC;

R_{pout} the outer radius of the primary ITC;

$R_{\sin}$ the inner radius of the secondary ITC;

R_{sout} the outer radius of the secondary ITC.

In Figs. 4 and 5, the primary and the secondary ITCs are presented in detail, respectively. In these figures, all the rings of each ITC are in series with each other. The symbols in these figures are as follows:

$g \cdot h$ the number of the rings in the primary ITC;

h the number of the layers in the primary ITC;

g the number of the rings in each layer of the primary ITC;

$p \cdot l$ the number of the rings in the secondary ITC;

l the number of the layers in the secondary ITC;

p the number of the rings in each layer of the secondary ITC;

d_w the diameter of the conductor;

H_{rp} the longitudinal distance between the rings of the primary ITC;

H_{zp} the latitudinal distance between the rings of the primary ITC;

H_{rs} the longitudinal distance between the rings of the secondary ITC;

H_{zs} the latitudinal distance between the rings of the secondary ITC.

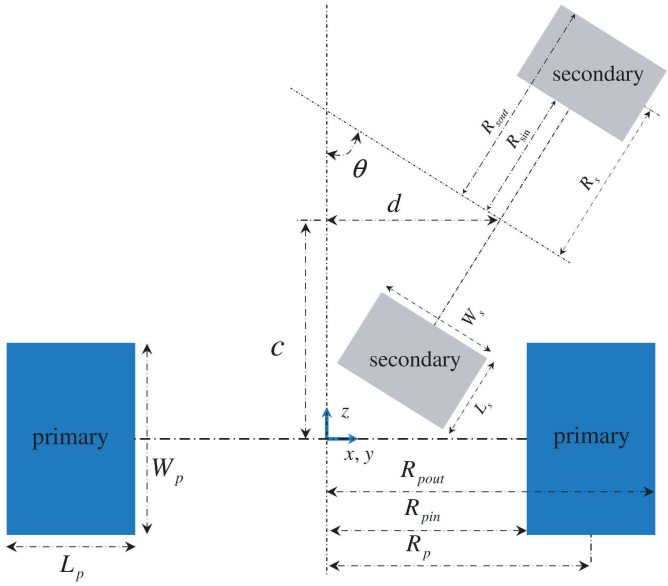

Figure 3. Two inclined circular ITCs with rectangular cross section (axes intersect but not at the center of one of the ITCs).

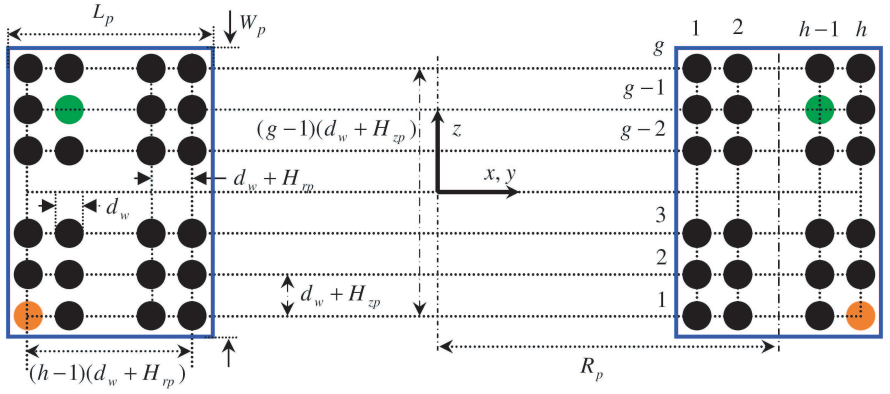

Figure 4. The primary filamentary circular ITCs in detail.

Note that all centers of the rings of the inclined secondary ITC lie in different points away from the axis of the primary ITC. Similarly, all centers of the rings of the primary ITC lie in different points away from the axis of the secondary ITC. The centers of these rings are on the same axes (see Figs. 4 and 5). In fact, in these arrangements we obtain a set of coupled filamentary inclined rings. So, it is necessary to make

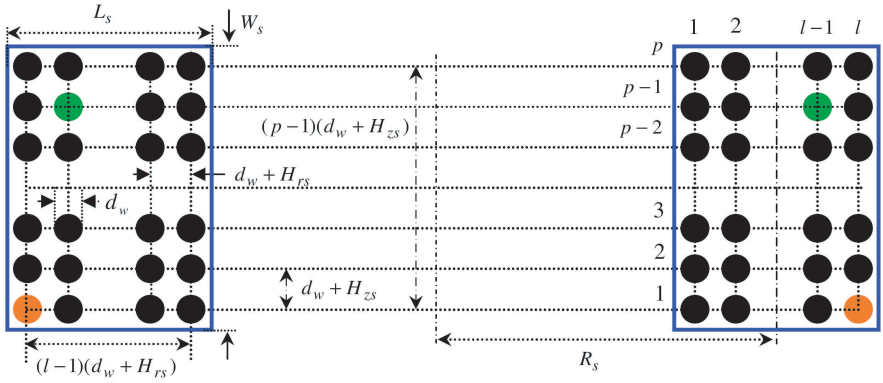

Figure 5. The secondary filamentary circular ITCs in detail.

some modifications in the filament method to take into consideration the different positions of the primary and the secondary rings which are, respectively, replaced by the primary and the secondary ITCs.

Thus, the mutual inductance between two inclined circular ITCs of rectangular cross section can be obtained in the following form:

$$M = \sum_{i=g_1}^{g_g} \sum_{j=h_1}^{h_h} \sum_{s=p_1}^{p_p} \sum_{t=l_1}^{l_l} M(i,j,s,t) \tag{6}$$

where:

$$M(i,j,s,t) = \frac{\mu_0}{\pi} \sqrt{R_p(j) R_s(t)} \cdot \int_0^{\pi} \left[\cos\theta - \frac{y(s)}{R_s(t)} \cos\varphi \right] \Psi(k_m) V_m^{-1.5} d\varphi \tag{7}$$

$$V_m = \sqrt{1 - \cos^2\varphi \sin^2\theta - 2\frac{y(s)}{R_s(t)} \cos\varphi \cos\theta + \left(\frac{y(s)}{R_s(t)} \right)^2} \tag{8}$$

$$\alpha_m = \frac{R_s(t)}{R_p(j)}, \quad \beta_m = \frac{z(i,s)}{R_p(j)}, \quad k_m^2 = \frac{4\alpha_m V_m}{(1+\alpha_m V_m)^2 + \xi_m^2} \tag{9}$$

$$\Psi(k_m) = \left(\frac{2}{k_m} - k_m \right) K(k_m) - \frac{2}{k_m} E(k_m) = Q_{1/2}(x_m), \tag{10}$$

$$y(s) = d + \frac{W_s \sin\theta}{p} s, \quad x_m = \frac{2 - k_m^2}{k_m^2} \tag{11}$$

$$\xi_m = \beta_m - \alpha_m \cos\varphi \sin\theta \tag{12}$$

$$R_p(j) = R_p + \frac{L_p}{h} j, \quad R_p = 0.5(R_{pout} + R_{pin}), \tag{13}$$

$$L_p = R_{pout} - R_{pin} = h(H_{rp} + d_w),$$
$$W_p = g(H_{zp} + d_w)$$
$$R_s(t) = R_s + \frac{L_s}{l}t, \quad R_s = 0.5(R_{sout} + R_{\sin}), \tag{14}$$
$$L_s = R_{sout} - R_{\sin} = l(H_{rs} + d_w),$$
$$W_s = p(H_{zs} + d_w)$$
$$z(i,s) = c - \frac{W_p}{g}i + \frac{W_s \cos\theta}{p}s \tag{15}$$
$$[l_1, l_2, \ldots, l_{l-1}, l_l]$$
$$= [-0.5(l-1), -0.5(l-1)+1, \ldots, 0.5(l-1)-1, 0.5(l-1)] \tag{16}$$
$$[p_1, p_2, \ldots, p_{p-1}, p_p]$$
$$= [-0.5(p-1), -0.5(p-1)+1, \ldots, 0.5(p-1)-1, 0.5(p-1)] \tag{17}$$
$$[h_1, h_2, \ldots, h_{h-1}, h_h]$$
$$= [-0.5(h-1), -0.5(h-1)+1, \ldots, 0.5(h-1)-1, 0.5(h-1)] \tag{18}$$
$$[g_1, g_2, \ldots, g_{g-1}, g_g]$$
$$= [-0.5(g-1), -0.5(g-1)+1, \ldots, 0.5(g-1)-1, 0.5(g-1)] \tag{19}$$

4. CONFIRMATION OF ANALYTICAL RESULTS USING FEM

The FEM is a numerical and computer-based technique for solving a variety of practical engineering problems that arise in different fields. It is recognized by developers and users as one of the most powerful numerical analysis tools ever devised to analyze complex problems in engineering. Because of its diversity and flexibility as an analytical tool, it is receiving much attention in engineering schools and in industry [30].

In this section, the mutual inductance between two ITCs are obtained using FEM when one of the dimensional parameters (H_{rp}, H_{zp}, C) are varied. Also, the real depth of penetration of two series ITCs versus frequency is obtained using FEM in the presence of a traveling plane electromagnetic wave. Then, the obtained results are compared with the corresponding analytical results. Fig. 6 shows the implemented model of two ITCs using FEMM software. As seen in this figure, because the ITCs have a symmetrical axis, it is enough to mesh only the half of the ITCs in FEM analysis. In this paper, non-uniform triangular meshing with open boundaries is used to simulate the experimental environment. The parameters of the ITCs are given in Table 1.

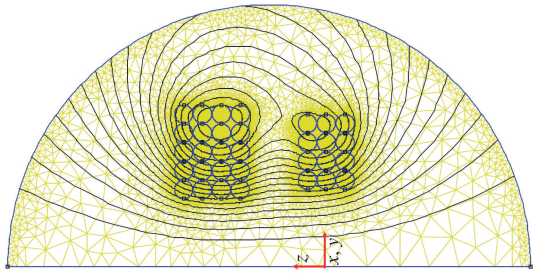

Figure 6. The implemented model of two series ITCs using FEMM software.

Table 1. The parameters of ITCS.

PARAMETERS OF THE PRIMARY ITC		PARAMETERS OF THE SECONDARY ITC	
g	3	p	4
h	4	l	5
H_{rp}	0.5 [mm]	H_{rs}	0.5 [mm]
H_{zp}	0.5 [mm]	H_{zs}	0.5 [mm]
L_p	66 [mm]	L_s	82.5 [mm]
W_p	49.5 [mm]	W_s	66 [mm]
R_p	100 [mm]	R_s	100 [mm]
$\sigma = 58$ [MS /m], $\varepsilon = 8.85$ [pF /m], $d = 0$ [mm]			
$\mu = 0.4\pi$ [μH /m], $d_w = 16$ [mm], $\theta = 0$ [rad]			

MATLAB® m-files are used to simulate the mutual inductance between two rings. Numerical integrations of Equation (1) are solved using the extended three-point Gaussian algorithm. The mutual inductance between two flat rings with $R_{ph} = 0.2\,[\mathrm{m}]$, $R_{sl} = 0.25\,[\mathrm{m}]$, $c_{gp} = 0.1\,[\mathrm{m}]$, $\theta = 0\,[\mathrm{rad}]$ and $y_p = 0\,[\mathrm{m}]$ using FEM result is calculated $0.2513\,[\mu\mathrm{H}]$ while the same inductance using the empirical result is calculated $0.24879\,[\mu\mathrm{H}]$ [31, 32]. The error resulting from the comparison between the empirical and the FEM result is calculated 0.01%. Additionally, the analytical result, which is obtained using Equation (1), shows an error of 0% when compared with the empirical result. Note that an "empirical result" is a formula based on observation experiments. In this paper, it means that other researchers have performed experiments in the laboratory and

developed a correlation between the inputs of the experiments and the outputs. So, the developed equations do not rely on basic science; they are just based on experimental works.

Figure 7 shows the magnetic flux density of two series ITCs when the current flowing through ITCs is 10 [KA]. As seen in this figure, the magnetic flux density is concentrated in the inner radius of the ITCs. Fig. 8 confirms this issue and shows that the magnetic flux density concentration occurs in the inner radius of the ITCs. Note that the magnetic flux density in Fig. 8 is drawn between two ITCs for $z = 50$ [mm].

Figure 9 and Table 2 compare the FEM and the analytical results of the mutual inductance between two ITCs versus L_p. The relation between L_p and H_{rp} is given in Equation (13). This figure shows that the mutual inductance decreases when H_{rp} increases. In other words, the inductive link between two ITCs decreases when L_p increases while R_p remains constant. This figure also shows that the decrease rate of mutual inductance in the inner rings of the primary ITC is much more than the increase rate of the mutual inductance in the outer rings of the primary ITC. The measured average error is less than 0.2043%. This error may be due to the mesh size and the computational error.

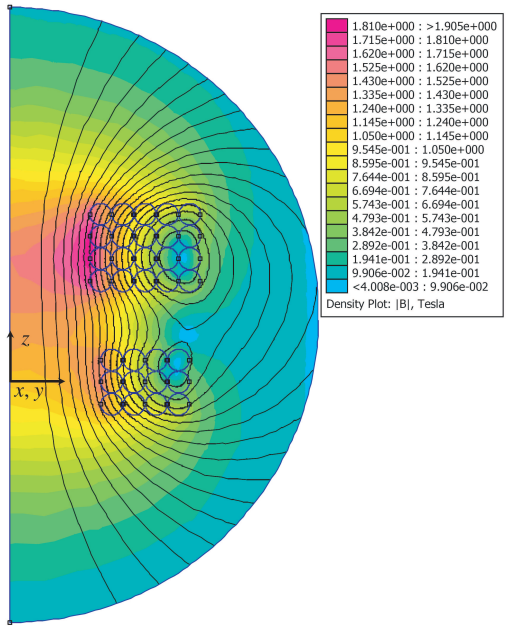

Figure 7. The magnetic flux density of two series ITCs in constant toroidal.

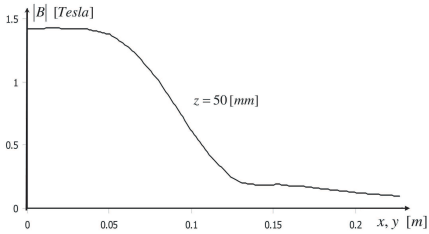

Figure 8. The magnetic flux density of two series ITCs in constant toroidal plane for $z = 50\,[\text{mm}]$.

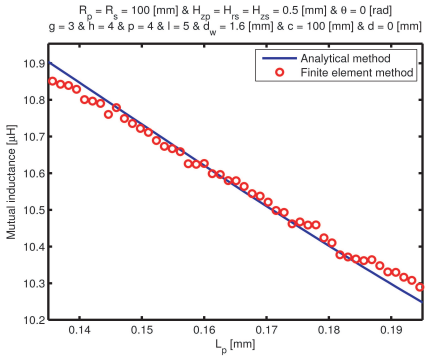

Figure 9. Comparing the FEM and the analytical results of the mutual inductance versus L_p.

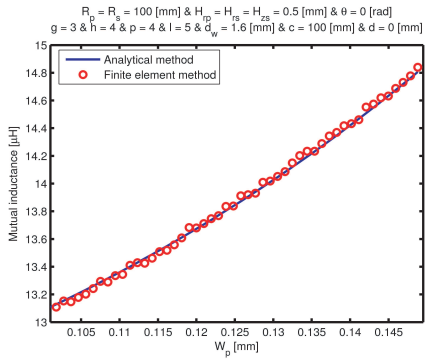

Figure 10. Comparing the FEM and the analytical results of the mutual inductance versus W_p.

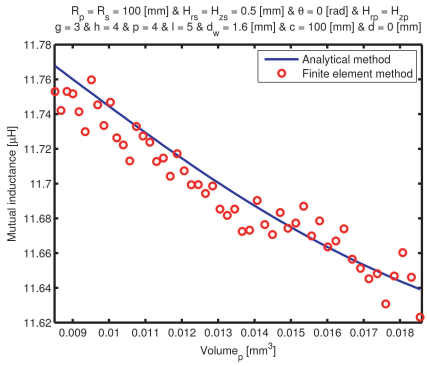

Figure 11. Comparing the FEM and the analytical results of the mutual inductance versus the volume of the primary ITC.

Figure 10 and Table 2 compare the FEM and the analytical results of the mutual inductance between two ITCs versus W_p. The relation between W_p and H_{zp} is given in Equation (14). This figure shows that the mutual inductance increases when H_{zp} increases. In other words, the inductive link between two ITCs increases when W_p increases while other parameters remain constant. From this figure it is also deduced that the increase rate of the mutual inductance in the upper rings of the primary ITC is much more than the decrease rate of the mutual inductance in the lower rings of the primary ITC. The measured average error is less than 0.1354%.

Figure 11 and Table 2 compare the FEM and the analytical results of the mutual inductance between two ITCs versus the volume of the primary ITC ($Volume_p$). The relation between $Volume_p$ and H_{zp} and H_{rp} is given in Equation (20). This figure shows that the mutual inductance decreases when $Volume_p$ increases. In other words, the more concentrated the primary ITC, the more mutual inductance between two ITCs. The measured average error is less than 0.0815%.

$$Volume_p = 2\pi R_p L_p W_p = 2\pi R_p g h (H_{rp} + d_w)(H_{zp} + d_w) \qquad (20)$$

Table 2. Comparing the FEM and the analytical results of the mutual inductance.

The mutual inductance [μH] versus L_p [mm]			The mutual inductance [μH] versus W_p [mm]			The mutual inductance [μH] versus $Volume_p$ [mm^3]		
L_p	*Analyt.*	*FEM*	W_p	*Analyt.*	*FEM*	$Volume_p$	*Analyt.*	*FEM*
0.1344	10.9106	10.8558	0.1008	13.1034	13.0959	0.0085	11.7678	11.7531
0.1357	10.8962	10.8512	0.1018	13.1289	13.1091	0.0087	11.7652	11.7422
0.1370	10.8817	10.8428	0.1027	13.1547	13.1530	0.0088	11.7626	11.7531
0.1382	10.8671	10.8395	0.1037	13.1808	13.1472	0.0090	11.7600	11.7518
0.1395	10.8526	10.8291	0.1046	13.2073	13.1789	0.0092	11.7574	11.7415
0.1408	10.8381	10.8010	0.1056	13.2340	13.2024	0.0093	11.7548	11.7299
0.1421	10.8236	10.7967	0.1066	13.2610	13.2427	0.0095	11.7521	11.7598
0.1434	10.8090	10.7907	0.1075	13.2884	13.2942	0.0097	11.7495	11.7454
0.1446	10.7945	10.7605	0.1085	13.3161	13.2898	0.0099	11.7468	11.7335
0.1459	10.7800	10.7789	0.1094	13.3441	13.3361	0.0100	11.7441	11.7469
0.1472	10.7655	10.7494	0.1104	13.3724	13.3452	0.0102	11.7413	11.7264
0.1485	10.7509	10.7358	0.1114	13.4011	13.4109	0.0104	11.7386	11.7223
0.1498	10.7364	10.7225	0.1123	13.4301	13.4291	0.0106	11.7359	11.7131
0.1510	10.7219	10.7117	0.1133	13.4594	13.4254	0.0108	11.7331	11.7330
0.1523	10.7075	10.6893	0.1142	13.4891	13.4619	0.0109	11.7303	11.7274
0.1536	10.6930	10.6736	0.1152	13.5191	13.5093	0.0111	11.7276	11.7239
0.1549	10.6785	10.6671	0.1162	13.5494	13.5193	0.0113	11.7248	11.7128
0.1562	10.6641	10.6590	0.1171	13.5801	13.5579	0.0115	11.7220	11.7148
0.1574	10.6497	10.6261	0.1181	13.6111	13.6082	0.0117	11.7193	11.7043
0.1587	10.6353	10.6243	0.1190	13.6425	13.6836	0.0119	11.7165	11.7172
0.1600	10.6210	10.6267	0.1200	13.6742	13.6806	0.0121	11.7137	11.7075
0.1613	10.6067	10.5989	0.1210	13.7063	13.7119	0.0123	11.7109	11.6994
0.1626	10.5924	10.5967	0.1219	13.7388	13.7475	0.0125	11.7082	11.6995
0.1638	10.5782	10.5802	0.1229	13.7716	13.7683	0.0126	11.7054	11.6944
0.1651	10.5639	10.5798	0.1238	13.8047	13.8360	0.0128	11.7027	11.6987

0.1664	10.5498	10.5640	0.1248	13.8383	13.8389	0.0130	11.6999	11.6854
0.1677	10.5356	10.5445	0.1258	13.8722	13.9126	0.0132	11.6972	11.6818
0.1690	10.5216	10.5379	0.1267	13.9065	13.9207	0.0135	11.6945	11.6854
0.1702	10.5075	10.5216	0.1277	13.9411	13.9316	0.0137	11.6918	11.6726
0.1715	10.4935	10.4986	0.1286	13.9762	14.0097	0.0139	11.6891	11.6733
0.1728	10.4796	10.4933	0.1296	14.0116	14.0185	0.0141	11.6864	11.6903
0.1741	10.4657	10.4623	0.1306	14.0474	14.0524	0.0143	11.6838	11.6765
0.1754	10.4519	10.4673	0.1315	14.0836	14.0865	0.0145	11.6812	11.6708
0.1766	10.4381	10.4588	0.1325	14.1202	14.1497	0.0147	11.6786	11.6834
0.1779	10.4244	10.4591	0.1334	14.1572	14.2023	0.0149	11.6760	11.6744
0.1792	10.4107	10.4241	0.1344	14.1946	14.2343	0.0151	11.6734	11.6774
0.1805	10.3971	10.4103	0.1354	14.2323	14.2343	0.0153	11.6709	11.6870
0.1818	10.3836	10.3776	0.1363	14.2706	14.2897	0.0156	11.6684	11.6699
0.1830	10.3701	10.3719	0.1373	14.3092	14.3442	0.0158	11.6660	11.6786
0.1843	10.3567	10.3663	0.1382	14.3482	14.3702	0.0160	11.6635	11.6637
0.1856	10.3434	10.3619	0.1392	14.3877	14.4183	0.0162	11.6611	11.6671
0.1869	10.3301	10.3643	0.1402	14.4276	14.4328	0.0165	11.6588	11.6741
0.1882	10.3169	10.3479	0.1411	14.4679	14.4613	0.0167	11.6564	11.6566
0.1894	10.3038	10.3309	0.1421	14.5086	14.5529	0.0169	11.6542	11.6513
0.1907	10.2908	10.3297	0.1430	14.5498	14.5743	0.0171	11.6519	11.6453
0.1920	10.2778	10.3165	0.1440	14.5914	14.6195	0.0174	11.6497	11.6482
0.1933	10.2649	10.3082	0.1450	14.6335	14.6328	0.0176	11.6475	11.6308
0.1946	10.2522	10.2896	0.1459	14.6760	14.6874	0.0178	11.6454	11.6469
0.1958	10.2394	10.2752	0.1469	14.7190	14.7305	0.0181	11.6433	11.6603
0.1971	10.2268	10.2804	0.1478	14.7625	14.7779	0.0183	11.6413	11.6462
0.1984	10.2143	10.2762	0.1488	14.8064	14.8404	0.0185	11.6393	11.6232

5. CONCLUSION

Detailed electromechanical analyses, including finite-element calculations, have been performed for hundreds of Tokamak designs including designs with round, D-shaped, and racetrack-shaped coils. In this paper, we derived analytic expressions for coil sets where the plane of the coil is tilted at an angle with respect to the radial plane.

The fundamentals of the analysis of mutual inductance presented in this study are helpful for the design and implementation of Tokamak reactors. This paper presented analytical equations of mutual inductance between two ITCs. These equations were solved using analytical and finite element methods. The MATLAB program was used for a numerical simulation of the mutual inductance, and the FEMM software was also employed for a magnetic analysis of two

ITCs. Comparing the analytical and the FEM results shows that the obtained errors is less than 0.2043%. Therefore, the proposed equations are highly reliable.

REFERENCES

1. Alexander, R. and P. Garabedian, "Choice of coils for a fusion reactor," *Proceedings of the National Academy of Sciences*, Vol. 104, No. 30, 12250–12252, Jul. 24, 2007.
2. Alizadeh Pahlavani, M. R. and A. Shoulaie, "A novel approach for calculations of helical toroidal coils inductance usable in reactor plasmas," *IEEE Trans. on Plasma Science*, Vol. 37, No. 8, 1593–1603, Aug. 2009.
3. Alizadeh Pahlavani, M. R. and A. Shoulaie, "Elimination of compressive stress in helical toroidal coils advanced structure for reactor plasmas," *IEEE Trans. on Plasma Science*, to be published.
4. Alizadeh Pahlavani, M. R. and A. Shoulaie, "Behavioral study of stress in toroidal, solenoidal, and helical toroidal coils with similar ring structures for reactor plasma," *International Review of Electrical Engineering*, Vol. 4, No. 1, 146–158, Jan.–Feb. 2009.
5. Alizadeh Pahlavani, M. R. and H. A. Mohammadpour, "Electromagnetic torque and force analysis of toroidal field coil using numerical and experimental results applicable to tokamak reactors," *IEEE Trans. on Plasma Science*, Vol. 38, No. 7, Jul. 2010.
6. Shiri, A., M. R. Alizadeh Pahlavani, and A. Shoulaie, "A new and fast procedure for calculation of the magnetic forces between cylindrical coils," *International Review of Electrical Engineering*, Vol. 4, No. 5, Sept.–Oct. 2009.
7. Shiri, A., D. Esmaeil Moghadam, M. R. Alizadeh Pahlavani, and A. Shoulaie, "Finite element based analysis of magnetic forces between planar spiral coils," *Journal of Electromagnetic Waves and Applications*, Vol. 2, 311–317, May 2010.
8. Alizadeh Pahlavani, M. R., H. A. Mohammadpour, and A. Shoulaie, "Numerical and experimental analysis of modular toroidal coil inductance applicable to tokamak reactors," *IEEE Trans. on Plasma Science*, Vol. 38, No. 2, 113–120, Feb. 2010.
9. Babic, S. I. and C. Akyel, "New mutual inductance calculation of the magnetically coupled coils: Thin disk coil-thin wall solenoid," *Journal of Electromagnetic Waves and Applications*, Vol. 20, No. 10, 1281–1290, 2006.

10. Akyel, C., S. I. Babic, and M.-M. Mahmoudi, "Mutual inductance calculation for noncoaxial circular air coils with parallel axes," *Progress In Electromagnetics Research*, Vol. 91, 287–301, 2009.
11. Akyel, C., S. I. Babic, S. Kincic, and J. P. Lagacé, "Magnetic force calculation between thin circular coils and thin filamentary circular coil in air," *Journal of Electromagnetic Waves and Applications*, Vol. 21, No. 9, 1273–1283, 2007.
12. Shiri, A. and A. Shoulaie, "A new methodology for magnetic force calculations between planar spiral coils," *Progress In Electromagnetics Research*, Vol. 95, 39–57, 2009.
13. Koledintseva, M. Y., J. L. Drewniak, T. P. Van Doren, D. J. Pommerenke, M. Cocchini, and D. M. Hockanson, "Method of edge currents for calculating mutual external inductance in a microstrip structure," *Progress In Electromagnetics Research*, Vol. 80, 197–224, 2008.
14. Koledintseva, M. Y., J. L. Drewniak, T. P. Van Doren, D. J. Pommerenke, M. Cocchini, and D. M. Hockanson, "Mutual external inductance in stripline structures," *Progress In Electromagnetics Research*, Vol. 80, 349–368, 2008.
15. Ravaud, R., G. Lemarquand, and V. Lemarquand, S. I. Babic, and C. Akyel, "Mutual inductance and force exerted between thick coils," *Progress In Electromagnetics Research*, Vol. 102, 367–380, 2010.
16. Conway, J. T., "Inductance calculations for noncoaxial coils using Bessel functions," *IEEE Trans. Magn.*, Vol. 43, No. 3, 1023–1034, Mar. 2007.
17. Zhao, P. and H.-G. Wang, "Resistances and inductances extraction using surface integral equation with the acceleration of multilevel green function interpolation method," *Progress In Electromagnetics Research*, Vol. 83, 43–54, 2008.
18. Wang, H.-G. and P. Zhao, "Combining multilevel Green's function interpolation method eith volume loop bases for inductance extraction problems," *Progress In Electromagnetics Research*, Vol. 80, 225–239, 2008.
19. Babic, S. I. and C. Akyel, "New analytic-numerical solutions for the mutual inductance of two coaxial circular coils with rectangular cross section in air," *IEEE Trans. Magn.*, Vol. 42, No. 6, 1661–1669, Jun. 2006.
20. Babic, S. I. and C. Akyel, "Improvement in calculation of the self- and mutual inductance of thin-wall solenoids and disk coils," *IEEE Trans. Magn.*, Vol. 36, No. 4, 1970–1975, Jul. 2000.

21. Akyel, C., S. I. Babic, and S. Kincic, "New and fast procedures for calculating the mutual inductance of coaxial circular coils (disk coil-circular coil)," *IEEE Trans. Magn.*, Vol. 38, No. 5, 2367–2369, Sep. 2002.
22. Babic, S. I., C. Akyel, and S. J. Salon, "New procedures for calculating the mutual inductance of the system: Filamentary circular coil-massive circular solenoid," *IEEE Trans. Magn.*, Vol. 39, No. 3, 1131–1134, May 2003.
23. Babic, S. I., S. Salon, and C. Akyel, "The mutual inductance of two thin coaxial disk coils in air," *IEEE Trans. Magn.*, Vol. 40, No. 2, 822–825, Mar. 2004.
24. Akyel, C., S. I. Babic, K. Wu, and F. J. Mojca, "Improvement in the mutual inductance calculation of thin coaxial circular coils with constant current density in air," *WSEAS Trans. Commun.*, Vol. 5, No. 6, 970–977, 1109–2742, Jun. 2006.
25. Babic, S. I. and C. Akyel, "An improvement in the calculation of the self inductance of thin disk coils with air-core," *WSEAS Trans. Circ. Syst.*, Vol. 3, No. 8, 1621–1626, Oct. 2004.
26. Akyel, C. and S. I. Babic, "Improvement in the mutual inductance calculation between coaxial circularcoils of rectangular cross section and thin coaxial circular coils with constant current density in air," *WSEAS Trans. Circuits Syst.*, Vol. 6, No. 5, 473–480, 1109–2734, May 2007.
27. Tang, W., X. He, T. Pan, and Y. L. Chow, "Synthetic asymptote formulas of equivalent circuit components of square spiral inductors," *Journal of Electromagnetic Waves and Applications*, Vol. 20, No. 2, 215–226, 2006.
28. Venkov, G., M. W. McCall, and D. Censor, "The theory of low-frequency wave physics revisited," *Journal of Electromagnetic Waves and Applications*, Vol. 21, No. 2, 229–249, 2007.
29. Pennington, R. H., *Introductory Computer Methods and Numerical Analysis*, 4th edition, Macmillan, New York, 1970.
30. Anderson, D. A., J. C. Tannehill, and R. H. Pletcher, *Computational Fluid Mechanics and Heat Transfer*, Hemisphere, Washington, DC, 1984.
31. Grover, F. W., *Inductance Calculation Working Formulas and Tables*, Chapter 11, 77–87, Dover Publications, Inc., New York, 1946.
32. Grover, F. W., *Inductance Calculation Working Formulas and Tables*, Chapter 16, 142–162, Dover Publications, Inc., New York, 1946.